Available online at www.sciencedirect.com
SCIENCE DIRECT®
Nuclear Instruments and Methods in Physics Research A 542 (2005) 81–86
NUCLEAR INSTRUMENTS & METHODS IN PHYSICS RESEARCH Section A
www.elsevier.com/locate/nima

Neutron-induced electron radiography

R. Pugliesi*, M.L.G. Andrade, M.A. Stanojev Pereira, F. Pugliesi

Instituto de Pesquisas Energéticas e Nucleares, IPEN—CNEN/SP, Av. Prof. Lineu Prestes 2242, Cidade Universitária, Butantã, CEP 05508-000, São Paulo-SP Brazil

Available online 2 February 2005

Abstract

In the present work, a new radiographic methodology which makes use of conventional X-ray films and low-energy electrons as penetrating radiation, to inspect low-thickness samples, has been investigated. The radiographic characteristics for the "electron beam–film" set, regarding its sensitivity to discern thickness changes of materials, as well as the spatial resolution achieved in the image have been determined. Some radiographs are presented and demonstrate the method's potential to inspect thin samples.

PACS: 81.70.−q

Keywords: Electron radiography; Thin layers

1. Introduction

There is a great scientific and technological interest to investigate the internal structure of low-thickness samples. The electron radiography as well as the auto-radiography are examples of some techniques which are available for such purposes. In the first, electrons emitted by a lead foil irradiated by X-rays pass through the sample. They are differentially absorbed in their passage and the specimen structure on a film is recorded. In the second, a radioactive material is inserted within the sample and the image is produced by putting the sample in contact with a film [1].

In the present methodology named "neutron-induced electron radiography-NIER", internal conversion electrons are employed as penetrating radiation [2]. As shown in Fig. 1, these electrons are emitted by a natural gadolinium metal foil under irradiation by thermal neutrons. Among the emitted electrons, the most important, for the purpose of the present paper, because of their higher intensities, are those with 70 keV [3], followed by the 150 keV with intensity 90% smaller [4]. The electrons emerging from the foil will be attenuated by the sample under inspection and the modulated transmitted intensity is registered by using a conventional X-ray film.

*Corresponding author. Tel.: +55 11 3816 9178; fax: +55 11 3816 9188.
E-mail address: pugliesi@curiango.ipen.br (R. Pugliesi).

0168-9002/$ - see front matter
doi:10.1016/j.nima.2005.01.015

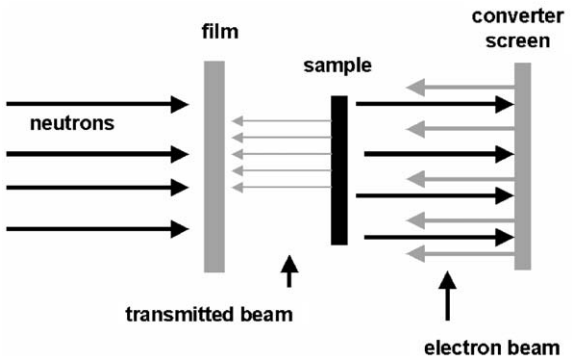

Fig. 1. Experimental set up.

The objective of the present work was to determine the radiographic characteristics of this "electron beam–film" set, in terms of its sensitivity to discern thickness changes of some materials as well as of the spatial resolution achieved in the image. In order to demonstrate the method's potential, several radiographs are presented in which the digital processing technique has been employed to improve image visualization [5].

2. Experimental

The gadolinium metal foil employed was 25 μm in thickness and was irradiated in a neutron radiography (NR) facility installed at the 2 MW, IEA–R1 pool-type Nuclear Research Reactor. The main characteristics of the neutron beam at the foil irradiation position are shown in Table 1 [6].

The radiographs were obtained by using an aluminum cassette inside which the film, sample and gadolinium metal foil (in this order with respect to the neutron beam) are kept in tight contact during irradiation. The neutron beam passes through the film, through the sample, and will induce (n,γ) reactions in the gadolinium metal foil. The generated electron beam reaches the sample and the transmitted intensity will sensitize the conventional X-ray film Kodak-AA, which was developed according to the standard procedures.

As proposed in this work, the following studies have been carried out:

Table 1
Characteristics of the neutron beam at the foil irradiation position

Thermal flux	1.7×10^{5} (n s^{-1} cm^{-2})
Neutron/gamma ratio	2.0×10^{6} (n cm^{-2} mRem^{-1})
Beam diameter	40 (cm)
Mean energy	7 (meV)

2.1. Sensitivity

The sensitivity of the "electron beam–film" set was defined here in terms of its capability to discern thickness changes of the materials. In order to evaluate it, it is necessary to determine the conditions in which the radiographs must be performed firstly. Such conditions are determined in terms of the best exposure and optical density intervals, for which the highest contrast is achieved in the image. For this purpose, the characteristic curve relating optical density-D_{op}, as a function of the beam exposure-E, has been determined. Optical density is defined as [7]

$$D_{op} = \log\left(\frac{I_o}{I}\right) \quad (1)$$

where I_o and I are the intensities of the incident and transmitted light through the film, respectively.

Since in the present work the electron beam was generated by a neutron beam, this curve has been obtained as a function of the neutron exposure-E (n/cm^2). Several film strips were irradiated and after their development, the optical density readings have been performed by using a standard optical densitometer having a minimal discernible optical density capability of 0.05. The obtained characteristic curve is shown in Fig. 2 and the highest contrast (indicated by arrows) was achieved for [8] 3×10^{7} n/cm^2 $<E<$ 1.2×10^{8} n/cm^2 and $1.3<D_{op}<3.5$.

The sensitivity has been determined for four materials. The samples are step wedges with thicknesses varying in the following range: adhesive tape –50 to 300 μm, aluminum foil −10 to 70 μm; polymer "Makrofol-KG" −10 to 100 μm; ordinary white paper −100 to 400 μm. These samples were radiographed and the behavior of

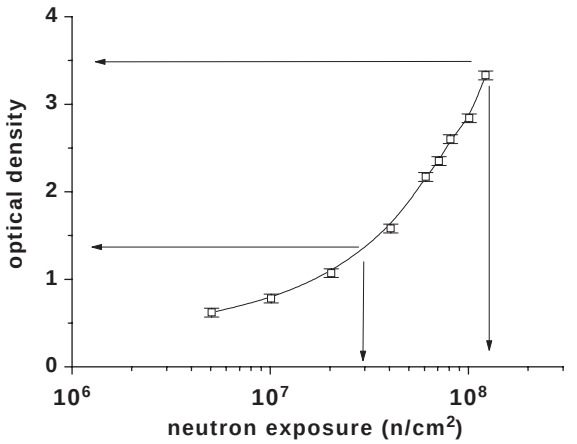

Fig. 2. Characteristic curve for Kodak-AA gadolinium metal foil set.

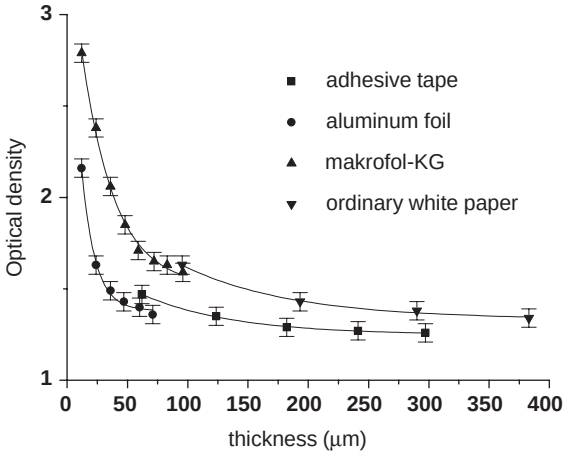

Fig. 3. Optical density behavior as a function of the sample thickness for the studied materials.

the optical density readings as a function of the sample thicknesses, are shown in Fig. 3. To these experimental data, the best fitted function was a first order exponential given by

$$D_{\mathrm{op}}(x) = A + B\,\mathrm{e}^{(-C\,x)} \tag{2}$$

where A, B, and C are free parameters in the fitting, and x is sample thickness.

The sensitivity was calculated from the derivative of (2) as

$$\Delta x = -\frac{\Delta D_{\mathrm{op}}\,\mathrm{e}^{(C\,x)}}{BC} \tag{3}$$

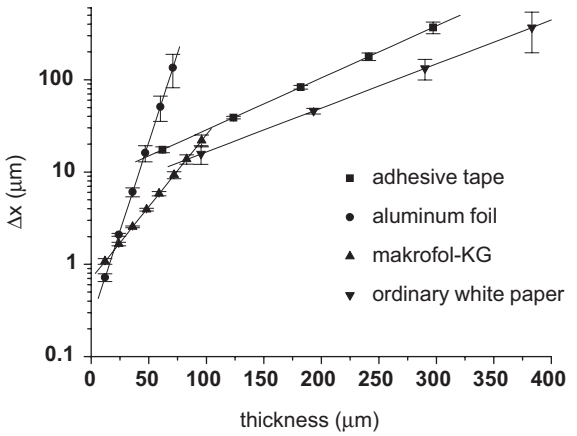

Fig. 4. Sensitivity behavior as a function of the sample thickness for the studied materials.

with $\Delta D_{\mathrm{op}} = 0.05$, being the minimal discernible optical density capability of the optical densitometer.

The plots of the sensitivity values as a function of the sample thicknesses are shown in Fig. 4.

2.2. Resolution

In radiography, the spatial resolution is defined as the minimal distance that two objects must be separated before they can be distinguished from each other [9]. The resolution is usually quoted in terms of the total unsharpness (U_{t}). In the present work, the total unsharpness has been obtained by scanning the optical density distribution at the interface between two images: the first corresponding to an electron opaque knife edge object (aluminum foil 100 μm), and the second to the direct electron beam. The scanning was performed by using a microphotometer having a light beam width of 3 μm and length of 700 μm. A typically obtained distribution is shown in Fig. 5. The following Edge Spread Function-ESF was fitted to this distribution [10,11]:

$$\mathrm{ESF} = p_1 + p_2 \arctan[p_3(X - p_4)] \tag{4}$$

where X is the scanning coordinate and p_1, p_2, p_3, and p_4, are free parameters in the fitting.

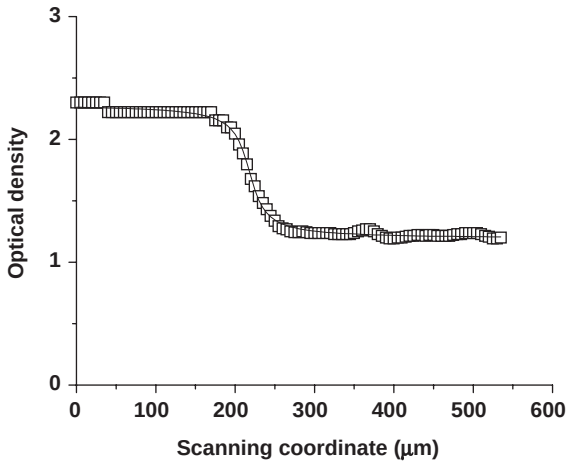

Fig. 5. Optical density distribution of a knife-edge object and the fitted edge spread function.

3. Analysis

As theoretically evaluated, more than 90% of the neutron beam is absorbed in the first 15 μm of the gadolinium foil. It has been calculated by using the well-known neutron transmission exponential law [12], and a microscopic cross section value of about 80,000 barn for the natural gadolinium, at the neutron energy of 7 meV [13]. Since the range of the most intense electrons (with energy of 70 keV), is about 20 μm, the "neutron–film–sample–gadolinium foil", irradiation geometry is justified and assures that most of the generated electrons will reach the sample.

The fitting of the exponential function (2) to the experimental data relating optical density as a function of the sample thickness is an empirical approach since the law governing the attenuation of the present electron beam, coming from the gadolinium foil, has not been determined.

As evaluated from (3), the method was able to discern ~20 μm of adhesive tape in 50 μm thickness, ~0.8 μm of aluminum foil in 10 μm thickness, ~1 μm of the polymer Makrofol-KG in 10 μm thickness, ~15 μm of ordinary paper in 100 μm thickness.

It is very important to note that after the maximum range of the 70 keV electrons is reached in the samples, the less intense 150 keV electrons will be the responsible for the image formation. In Table 2, the approximate values for the ranges for both energies, for the studied materials, are presented [14]. As can be seen in Fig. 3, the optical densities for aluminum foil and Makrofol-KG clearly decrease slower after the thickness of 40 and 70 μm, respectively. For adhesive tape and ordinary paper, only the 150 keV electrons will form the image since the minimal thickness of these samples, 50 and 100 μm, respectively, are near to the limit of the 70 keV electrons range. Together with the electrons, gamma-radiation is also emitted by the gadolinium foil. However, because of its high penetration in the present samples, its contribution to the image formation is just to increase the film background.

Table 2
Approximate values for the range of 70 and 150 keV electrons for the studied materials

Material	Range (μm) 70 keV	Range (μm) 150 keV
Aluminum foil	40	140
Makrofol-KG	70	240
Paper	60	210
Adhesive	80	270

The minimal detectable thickness or the minimal amount of material inserted in the beam able to be realized was also evaluated for each one of the studied materials. The obtained values presented in Table 3 have been calculated by extrapolating (3) to $x \to 0$. In order to show the high potential of the method, the approximate values for the minimal detectable thickness, evaluated for the standard neutron radiography technique by using the same film/foil set, for two materials, gadolinium and cadmium, which possess the two greatest thermal neutron capture cross section, are also presented in Table 3 [6,7].

Another important aspect of this technique is the high resolution achieved in the image. The total unsharpness calculated by Eq. (4) is given by $U_t = 2/(p_3)$" [6,10], and the obtained result was $U_t = (30 \pm 1)\,\mu$m. This high resolution is a consequence of several factors: the small sample thickness; the low range of the electrons in the film; since the samples were radiographed in a close contact with the film/foil set, the geometrical unsharpness contribution is negligible [8].

Although the employment of an evacuated cassette would improve the resolution of the images, it was not used in the present work because the wet samples like the plants, would be crashed between the converter and the film, causing damages in both.

It was also experimentally verified, for these samples, if a neutron image is superimposed to the resulting electron image. For such purpose, the same step wedges have been neutron radiographed at the same neutron exposure, by using the same converter film/foil combination. Since the differences on the optical density values, corresponding to steps of the samples with those for the direct electron beam, are smaller than 5%, its influence on the resulting electron image was considered negligible. In order to demonstrate the possible applications of this methodology, some selected samples have been radiographed. The obtained results are shown in Figs. 6 and 7 in which the standard digital processing procedures, to improve image visualization, have been employed. Fig. 6 shows a plant where it is easy to observe the presence of some nutrients inside the stems and Fig. 7 shows a regular Brazilian bill, where it is easy to observe one of the security marks [2].

Table 3
Comparison of the minimal detectable thickness between the NIER and the standard "NR" techniques

	Material	Min. thick.(μm)
NIER	Aluminum foil	0.25 ± 0.05
	Makrofol-KG	0.69 ± 0.07
	Paper	6 ± 2
	Adhesive	8 ± 1
NR	Gadolinium	0.2
	Cadmium	2

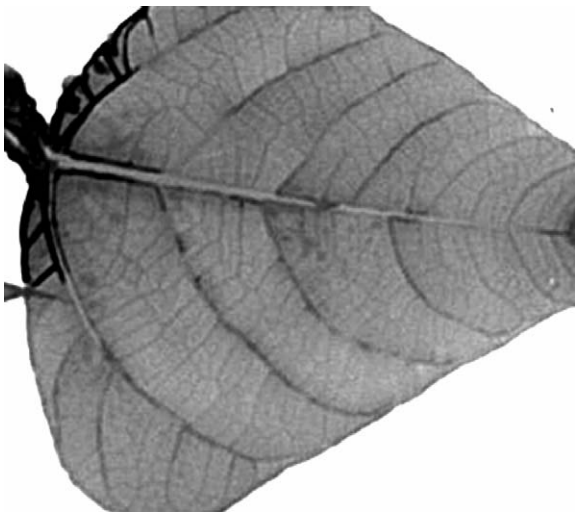

Fig. 6. Neutron-induced electron radiography of a plant showing some nutrients inside the central stem.

Fig. 7. Neutron-induced electron radiography of a regular Brazilian bill showing one of the security marks.

4. Conclusions

In principle, neutron-induced electron radiographs can be obtained in neutron radiography facilities, by making use of standard gadolinium screens and X-ray films. However, since the film is irradiated together with the screen, the beam's neutron/gamma ratio must be greater than $5 \times 10^5\,\mathrm{n\,cm^{-2}\,m\,Rem^{-1}}$ [7].

According to the obtained results the NIER is a promising technique, suitable to inspect low-thickness samples, with a capability to discern thickness changes on the order of microns, and a maximal resolution of about 30 μm.

Several other neutron-induced radiation radiography techniques can be also used. For example the employment of α-emitting boron-based converter screen combined with track-etch foils has

demonstrated to be useful to inspect lower thickness samples [2].

References

[1] Eastman Kodak Co., 1994–2003. Rochester, New York. Available in: http://www.kodak.com access in April 15, 2003.
[2] R. Pugliesi, Meeting of the Advisory Group for Development and Application of Neutron radiography. International Atomic Energy Agency (IAEA) Vienna, Austria, 1–4 October 2001.
[3] M.R. Hawkesworth, Atom. Energy Rev. 152 (1977) 169.
[4] National Nuclear Data Center. Brookhaven National Laboratory. Upton, NY 11973–5000 http://bnlnd2.dne.bnl.gv access in: November 04, 2003.
[5] K.R. Castleman, Prentice Hall Upper Saddle River, New Jersey, 1996, p. 07458.
[6] M.L.G. Andrade, M.Sc. Thesis. Nuclear Energy National Commission. IPEN-CNEN/SP, Brasil, 2002.
[7] H. Berger, NTIAC–SR–98–01. NASA (Center for Aerospace Information) 1998.
[8] P. Hardt, von Der, H. Roettger, Neutron Radiography Handbook: Nuclear Science and Technology, D. Reidl, Dordrecht, 1981.
[9] R. Ilic, M. Najzer, Nucl. Track Radiat. Meas. 17 (1990) 469.
[10] A.A. Harms, A. Zellinger, Phys. Med. Biol. 22 (1) (1977) 70.
[11] M. Wrobel, L. Greim, Geesthacht, GKSS, German, GKSS 88/e/12, 1988.
[12] L.F. Curtiss, D. van Nostrand Co. Inc., Princenton, New Jersey, 1959.
[13] D.J. Hughes, J.A. Harvey, McGRAW-Hill, New York, NY, 1955 (BNL-325).
[14] National Institute of Standards and Technology. Radiation Dosimetry Data http://physics.nist.gov/PhysRefData-radi.html accessed on 30 June 2003.